Twenty-five years of narrowband metal resonance lidars and current trends

Chiao-Yao She, Colorado State University
Currently visiting NIPR

Outline of the talk:

History: It began with temperature measurement in Europe

Doppler effect in resonance scattering (Laser Induced Fluorescence): Physics for narrowband metal resonance scattering lidars

In north America: measuring temperature and wind

Science example: Searching for the global mesopause thermal structure

CSU Na lidar investigating dynamics at different time scales

Current trends and directions on metal lidar technologies

Conclusion

Laser induced fluorescence: NaD_2-T-W measurement

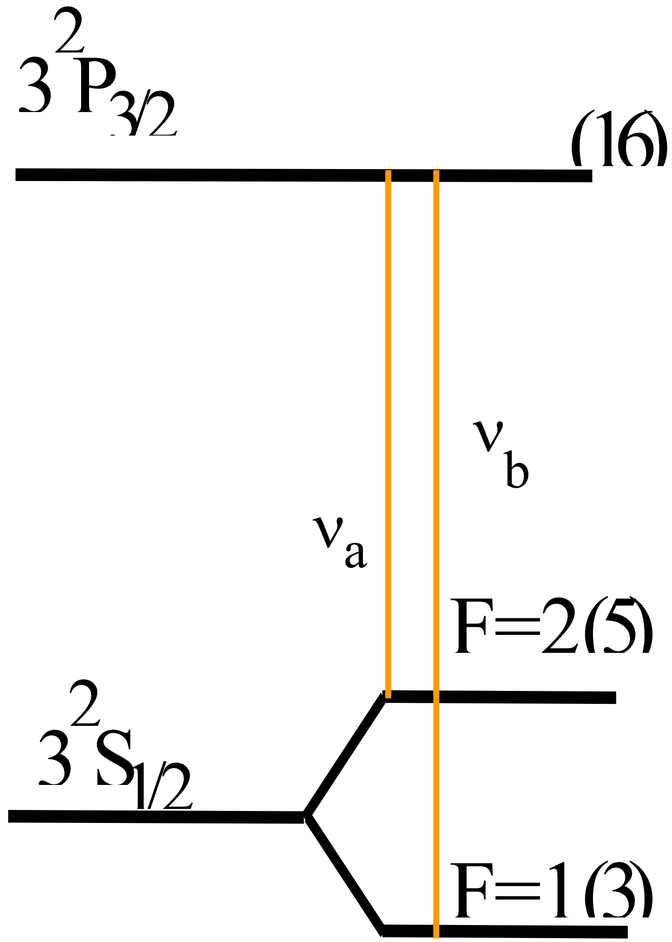

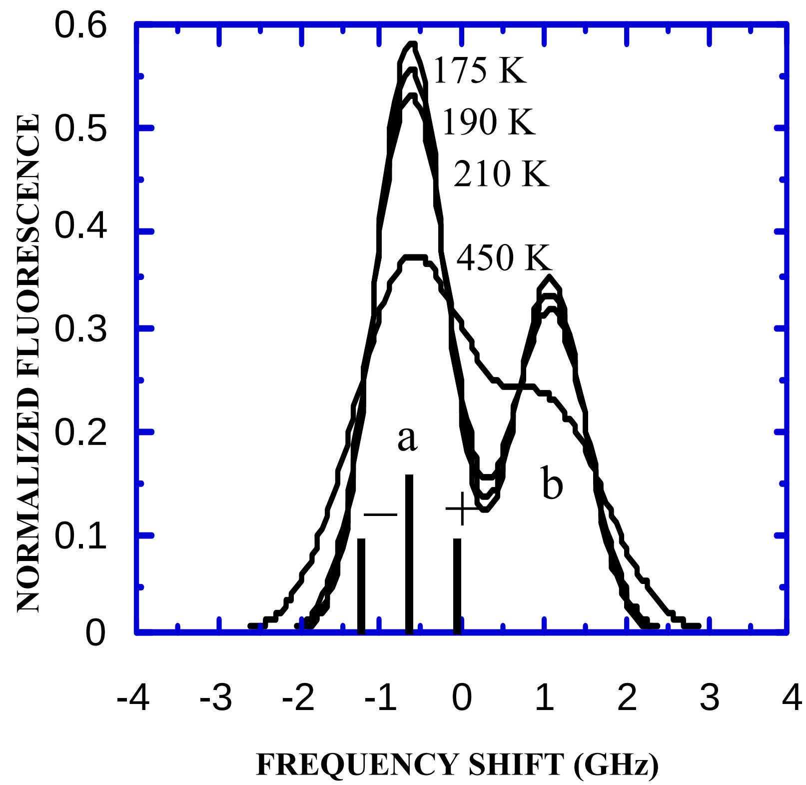

1nm ~ 1050 GHz; 1MHz ~ 0.6m/s

- **Scanning: Spectrum → temperature**
- $\mathbf{R_T = (I_+ + I_-) / 2I_a; R_W = (I_+ - I_-) / I_a}$

Historical temperature measurements

Demonstration of Doppler temperature measurement via a tunable dye laser
Nonlinear fit to spectrum

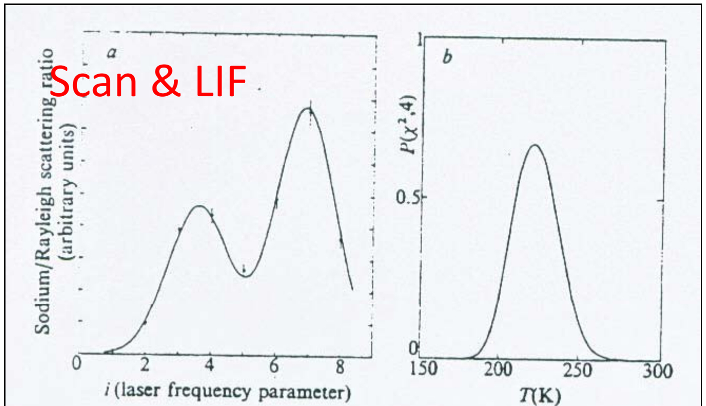

Fig. 1 *a*, Ratio of the sodium to Rayleigh scattered signals as a function of laser frequency for 1,200 laser shots on 30 January 1979, together with the theoretical lineshape which provides the best fit to the data. *b*, The probability $P(\chi^2, 4)$ as a function of temperature for the curve-fitting in *a*.

Gibson, Thomas, and Bhattachacharyya, Nature (1979)

Fricke and von Zahn, JATP (1985)

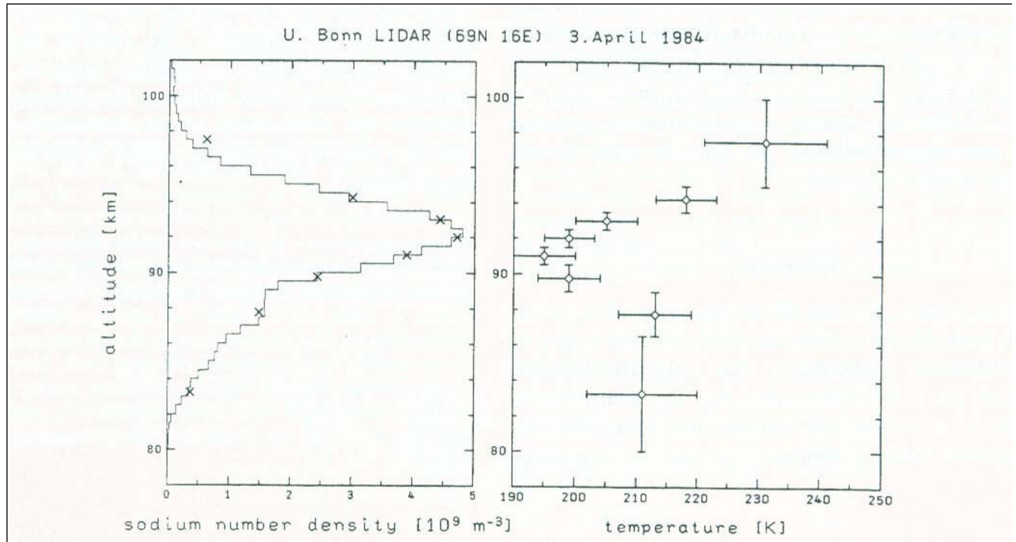

Fig. 8. Results obtained for 3 April 1984 between 21 h 06 m and 22 h 52 m UT at Andøya (69°N, 16°E). The sodium layer was subdivided into eight slices of about equal signal strength to obtain comparable signal/noise ratios throughout the layer. (a) Average sodium number densities in each of the eight slices (crosses). These are based on comparison with the Rayleigh scattered signal from 30 km altitude. The line is the solid angle corrected count rate, normalized to the sodium density in the 91 ± 0.5 km slice. Differences are mainly due to the different altitude resolution of the two datasets. (b) Mesospheric temperature profile. Note that the absolute value of the temperature scale is uncertain by about ± 10K because of the remaining uncertainty in the lineshape of the lidar transmitter. Error bars in the figure show statistical errors from the fit procedure only.

Five years of science observation with a number of excellent science publications plus climatoloy studies in Lübken/Zahn (1991)

Doppler Effect for LOS wind & temperature measurement with LIF works differently from that with Rayleigh scattering

Cabannes(Rayleigh) scattering :

$$\nu_{rec} = \nu_L (1 - \frac{2u}{c}) = \nu_L - \frac{2u}{\lambda_L}$$

Frequency analysis

(or with associated intensity)

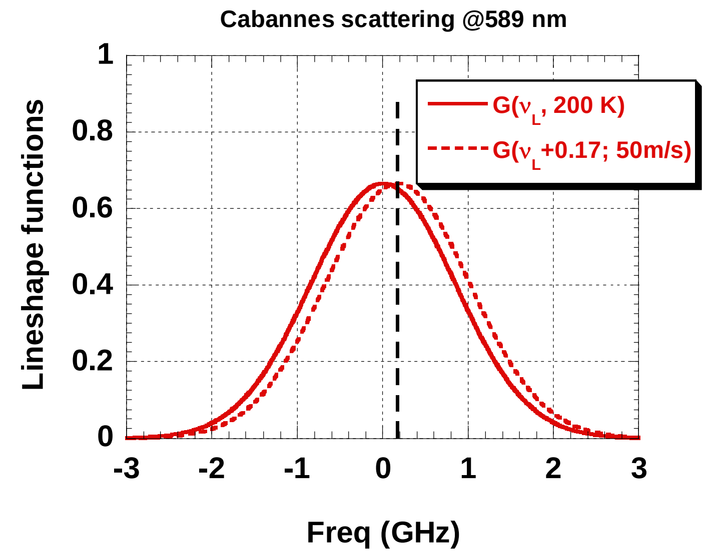

LIF=Absorption+Re-emssion

$$Abs: \nu_a = \nu_0 = \nu_L - \frac{u}{\lambda_0}; \text{Re-}emission:$$

$$\nu_e = \nu_0 - \frac{u}{\lambda_0} = \nu_0 - (\nu_L - \nu_0) = 2\nu_0 - \nu_L$$

Frequency analysis doesn't work

Intensity dependent T and LOS wind

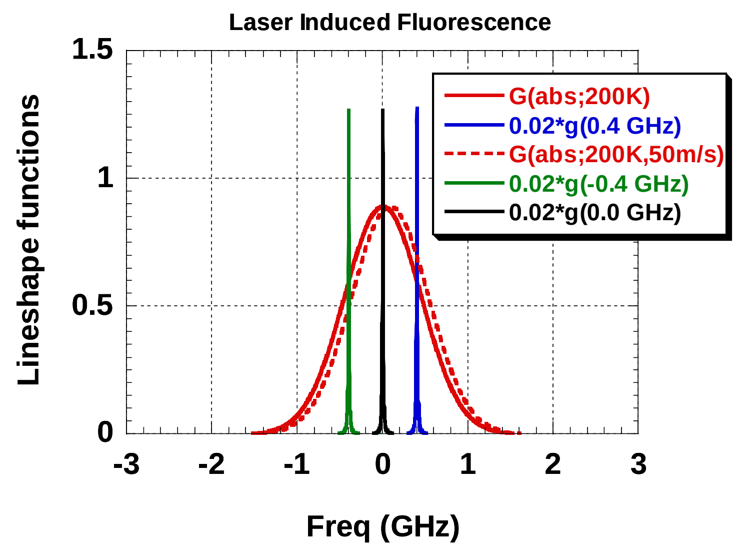

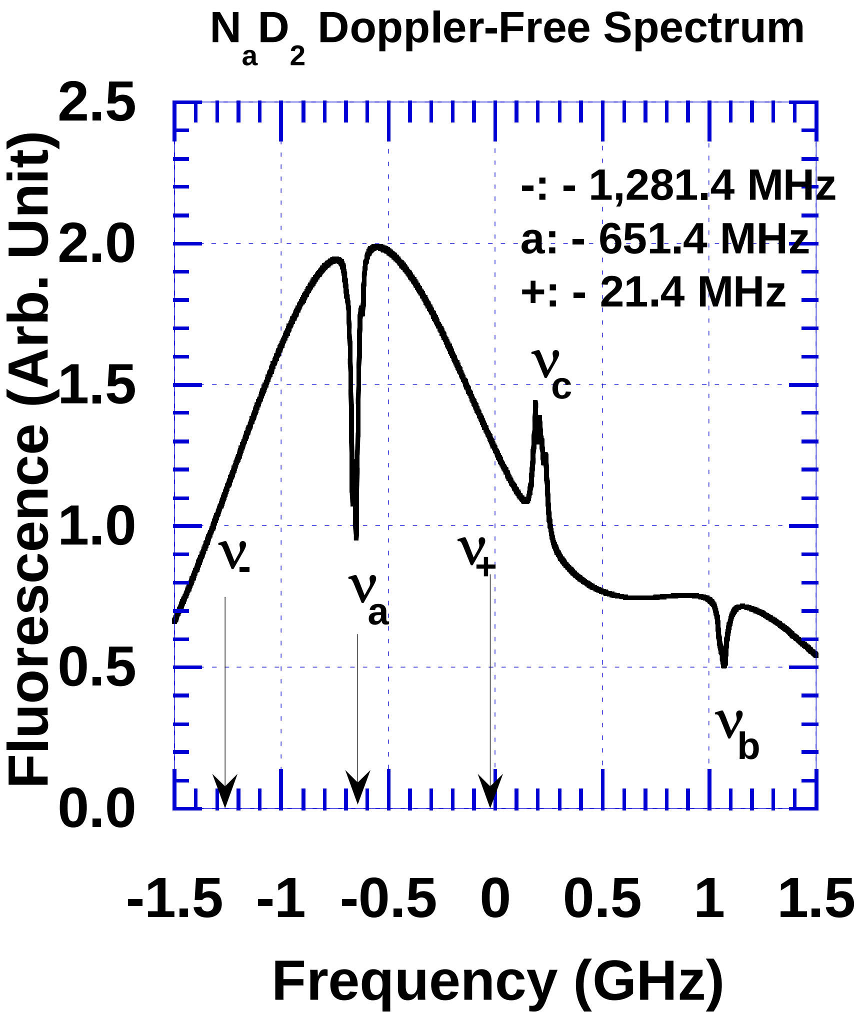

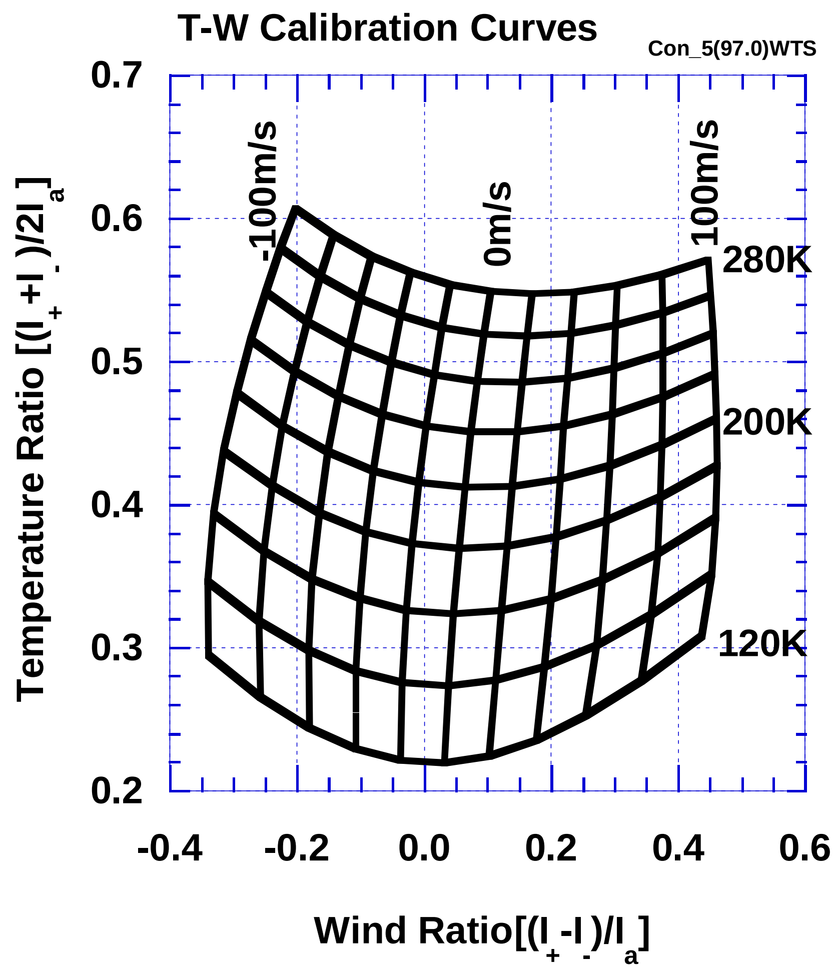

We use DFS to lock the laser at ν_a and AOM to get to ν_+ and ν_-

- $R_T = (I_+ + I_-) / 2I_a$
- $R_W = (I_+ - I_-) / I_a$

Observation Under Sunlit Conditions
Sodium Faraday Filter: Rejection of sky background

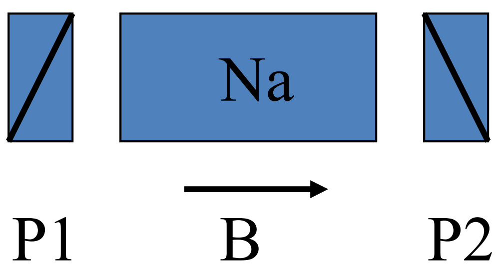

A heated sodium cell in axial magnetic field between two crossed polarizers

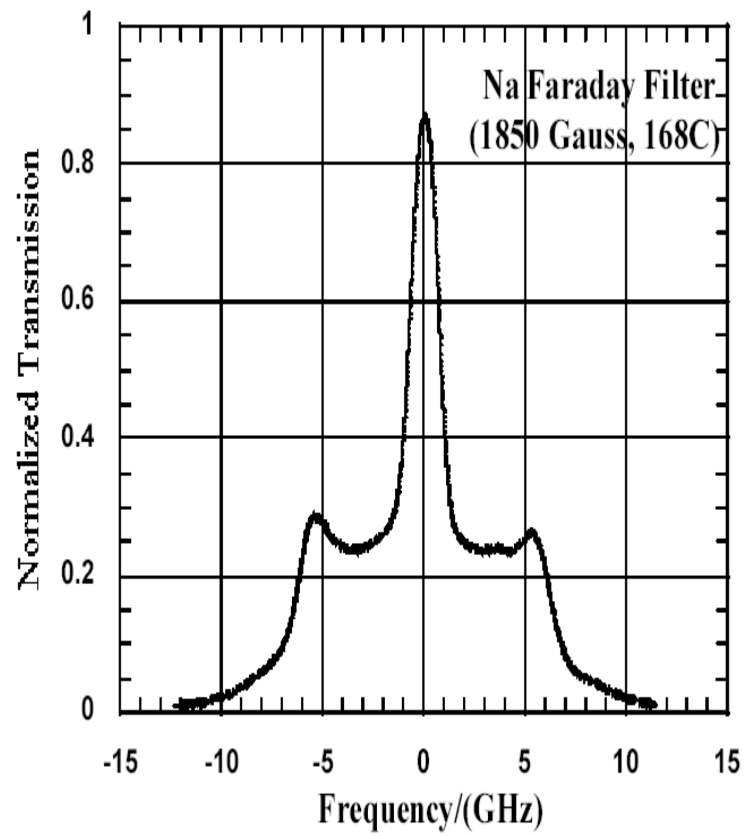

Chen et al., 1993 and 1996

Temp – Wind Obs. by Na lidar

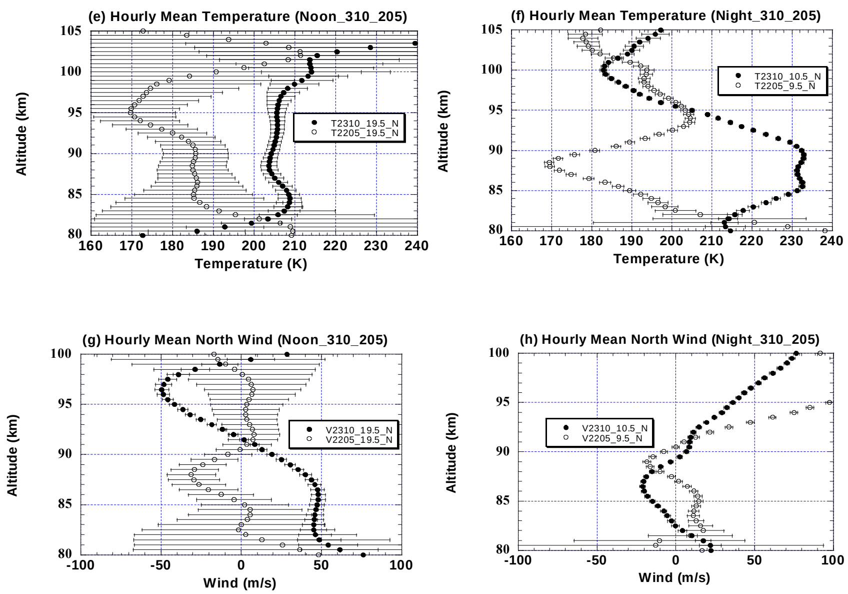

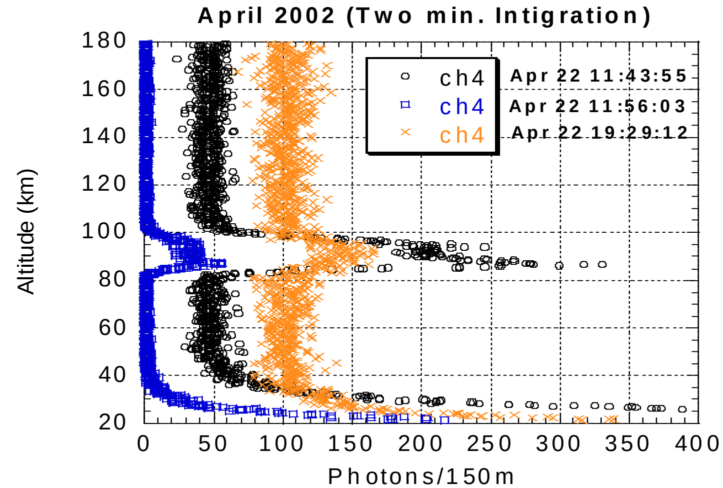

CSU hourly mean profiles in summer and winter at night (right) and noon (worst case; left) with respectively measured temperature profiles (upper panels) and wind profiles (lower panels).

The CSU Na lidar system in 2002 with two beams pointing 30^{o} off zenith, one to the east, the other to the north. Each beam has a telescope, 35 cm in diameter.

• Summer noon Range: 84-97km Delta: <20K,<30m/s	• Summer night Range: 84-100km Delta: <2K, <3m/s
• Winter noon Range: 82-98km Delta: <5K,<10m/s	• Winter night Range: 84-100km Delta: <1K, <2m/s

Measurement uncertainties of a scaled Na Lidar system with two 80cm diameter telescopes will be reduced by a factor of **2.3.**

Mesopause temperature structure: Double minima?

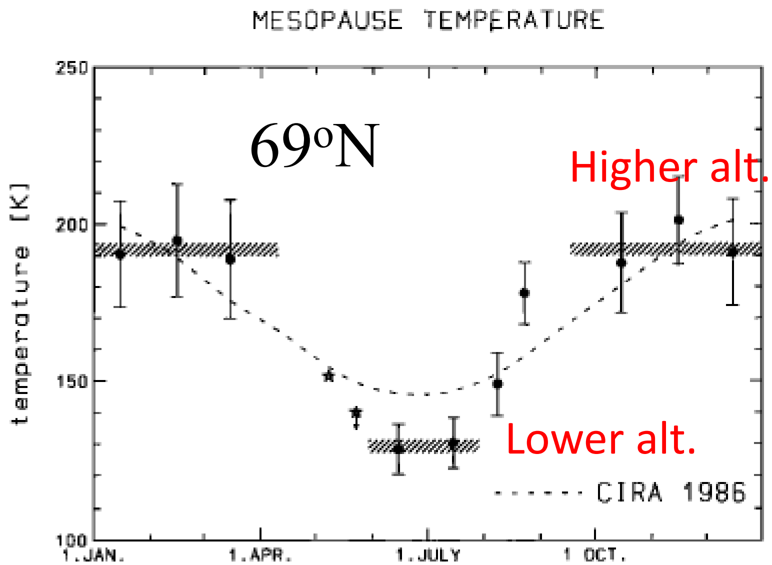

Lübken/Zahn (1991)

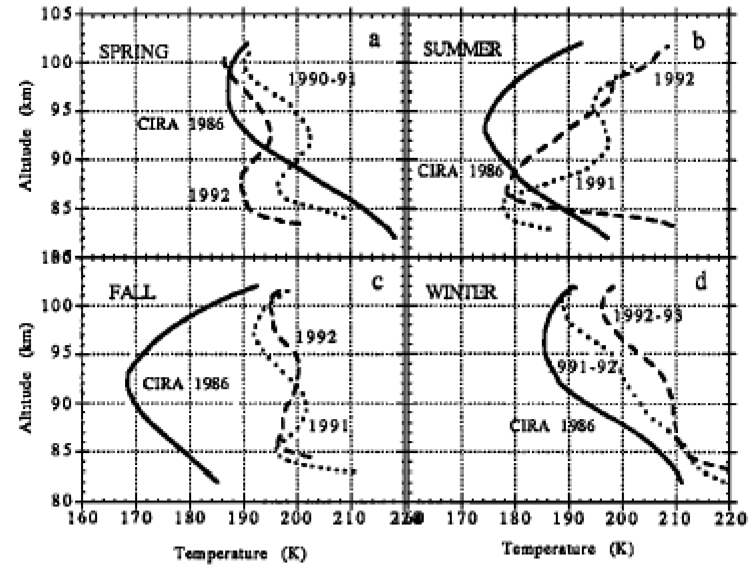

@ 41°N; She et al. (1993)

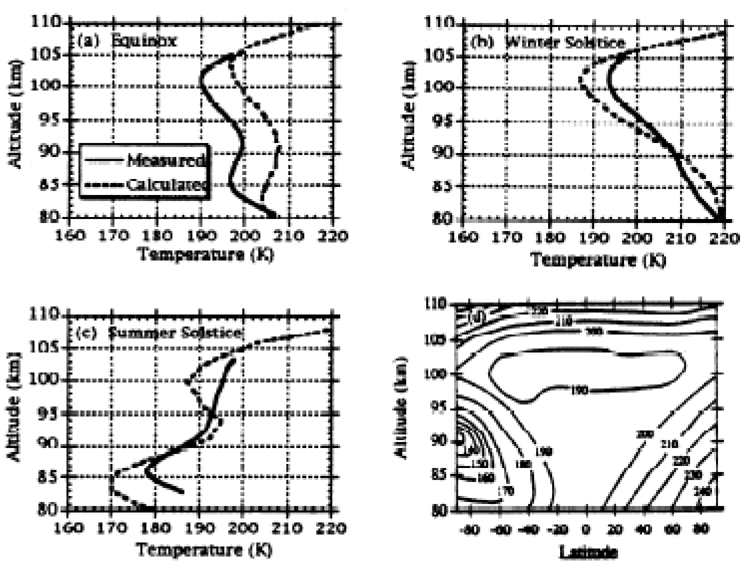

Agree with model; She et al. (1995)

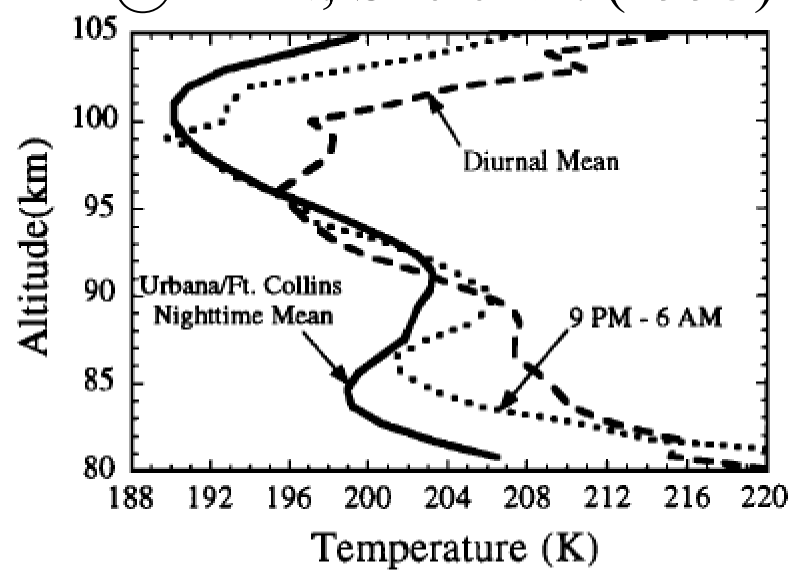

States and Gardner (1998)

Global mesopause thermal structure

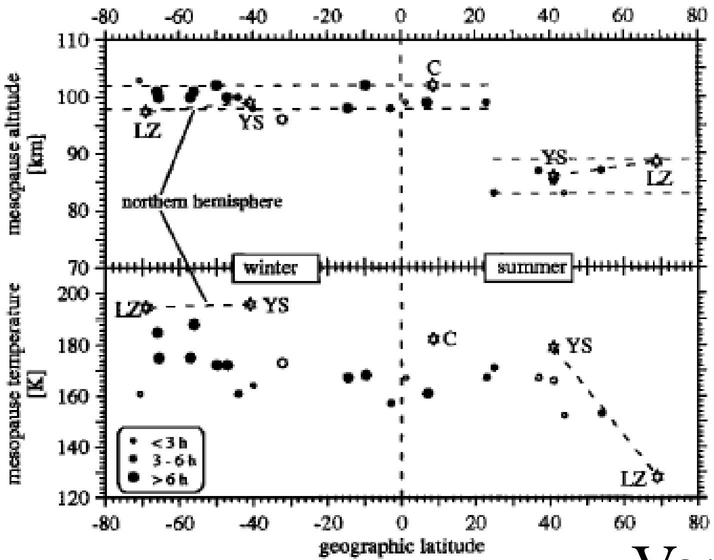

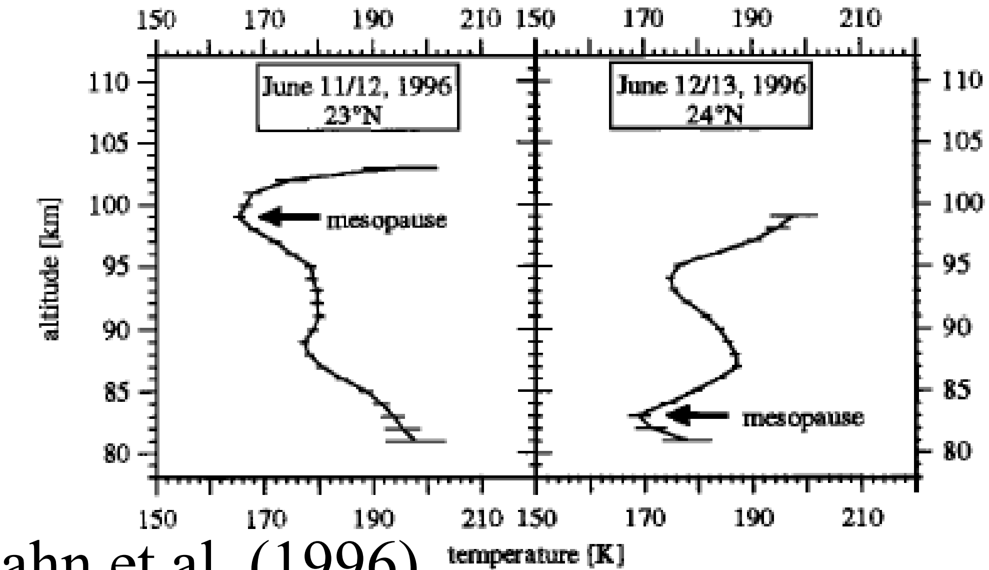

Von Zahn et al. (1996)

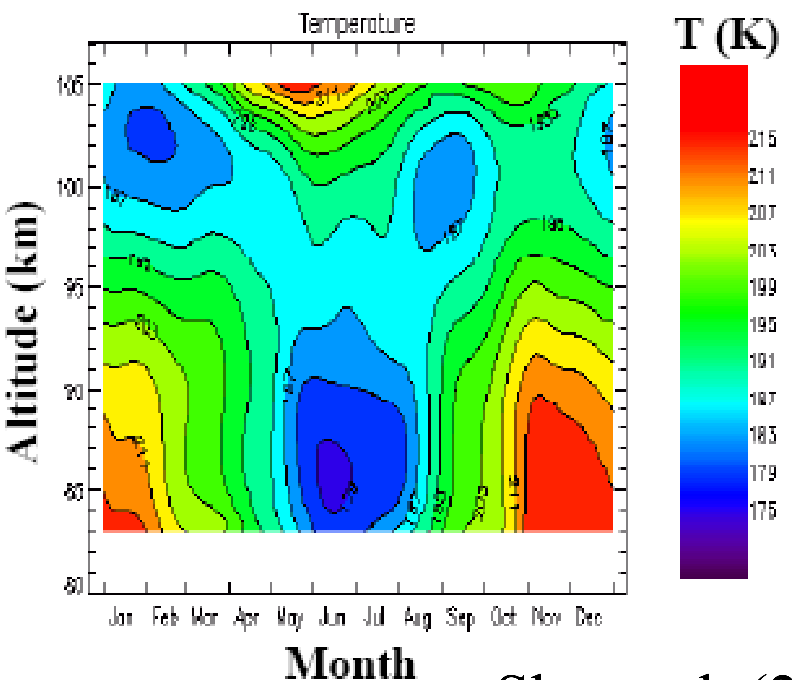

She et al. (2000)

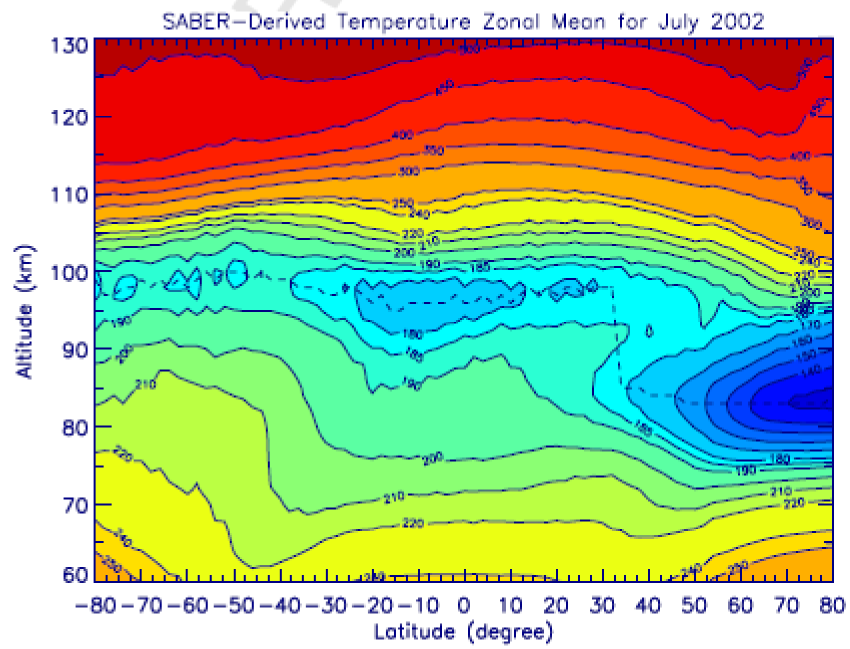

Mertens et al. (2000)

Tides and tidal variability – CSU Full-diurnal Lidar Observation (raw data)

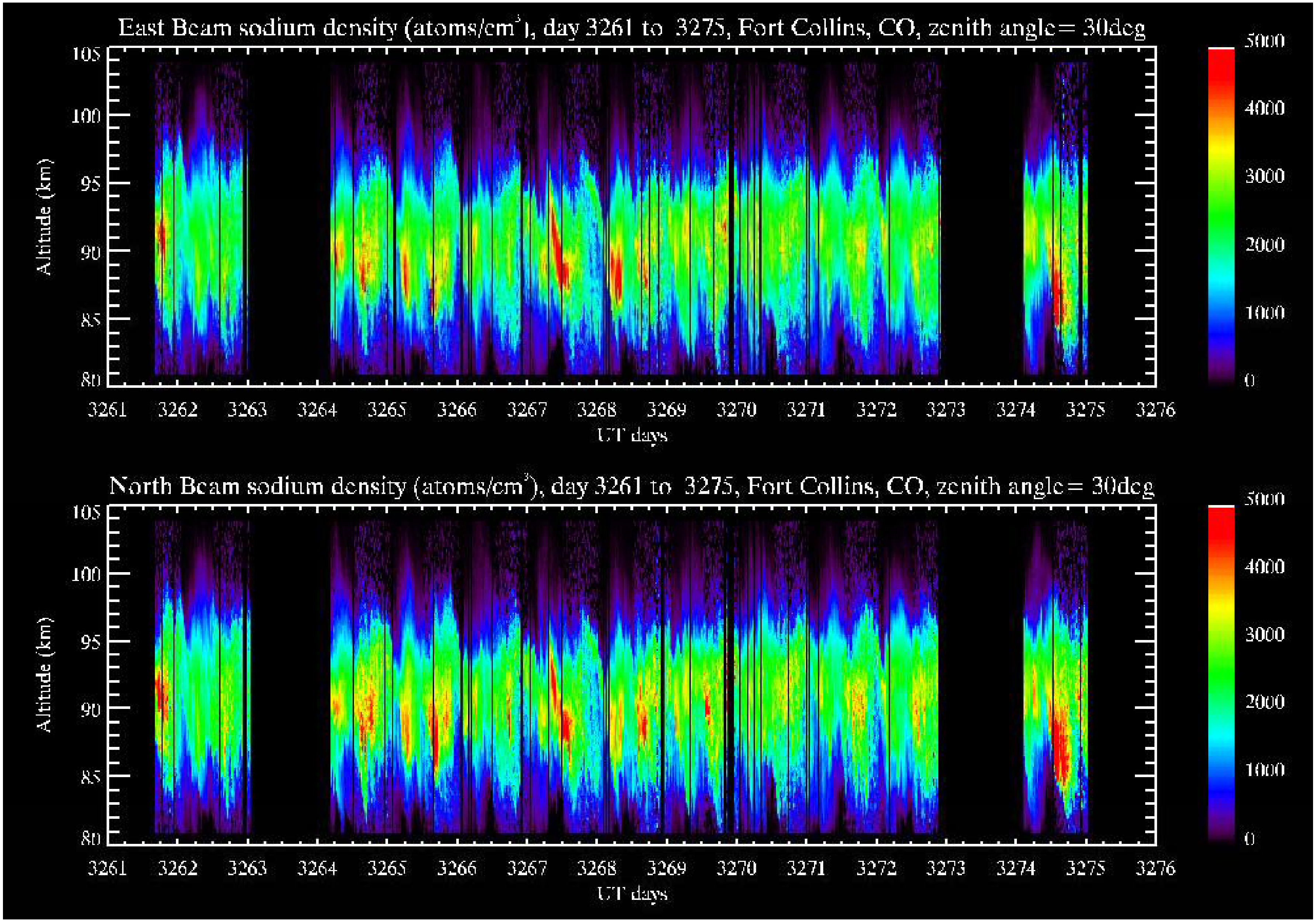

September 2003
Diurnal Cycle Observations

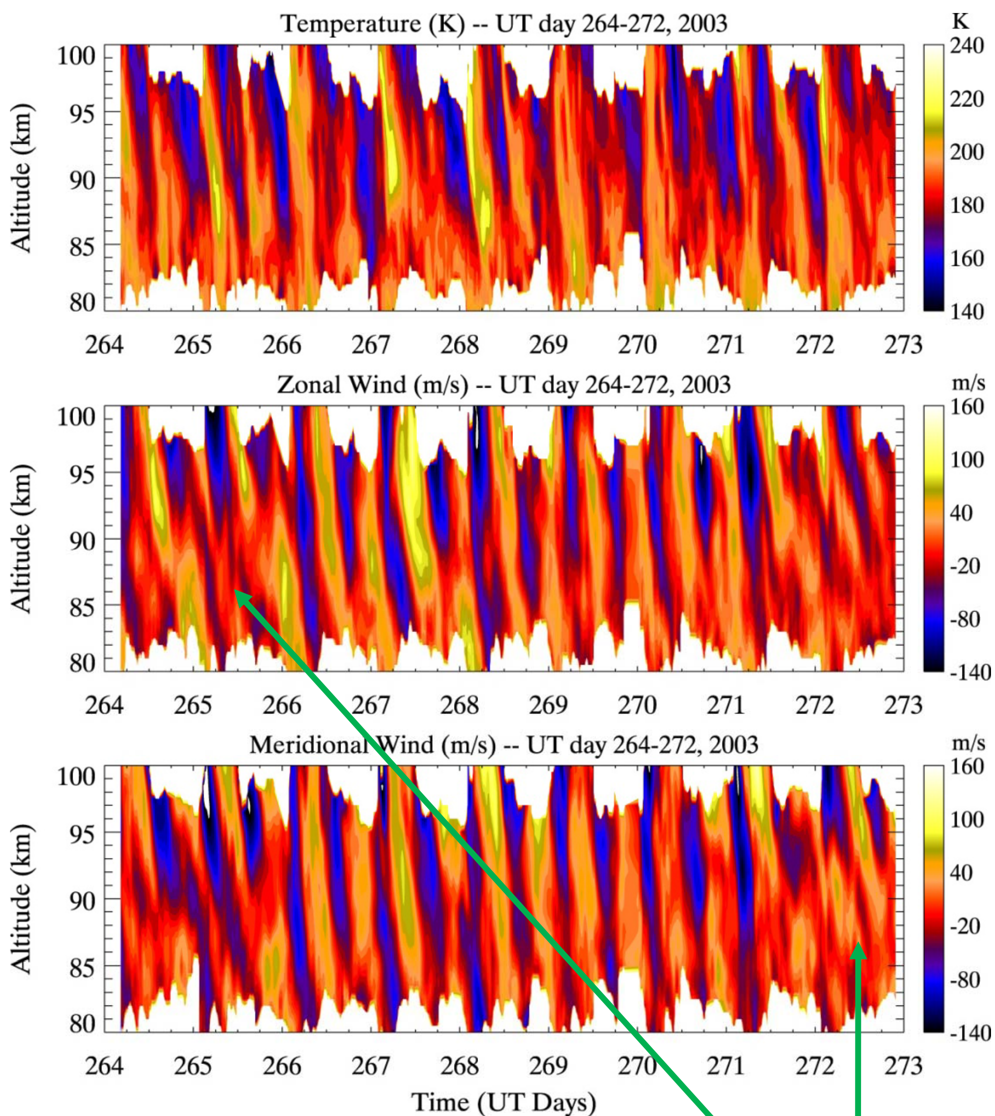

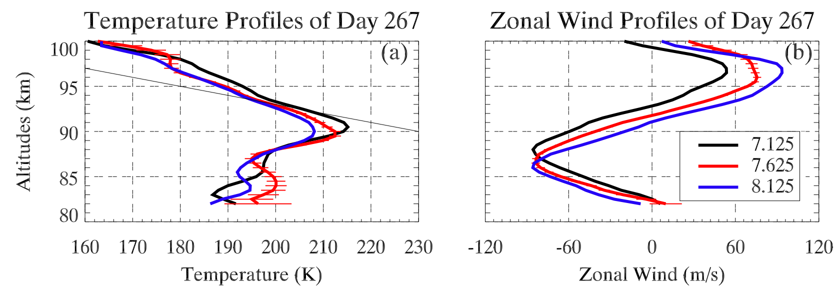

Convective instability; large wind grad.

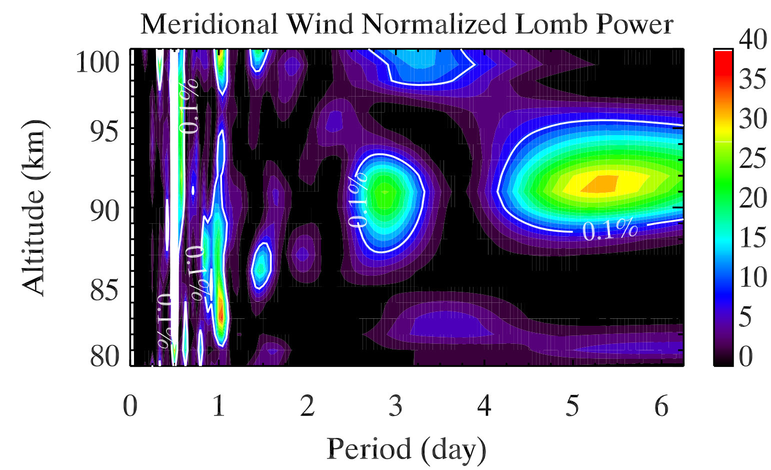

Planetary-tidal wave interactions

Nine-day continuous observation of
Tidal perturbations & variability; GWs

She et al., GRL, 2004

Mean state (T, U, V) and GCM comparison, Fig.4 of Yuan,S,K,S,G,R,L,&S; JGR, 2008

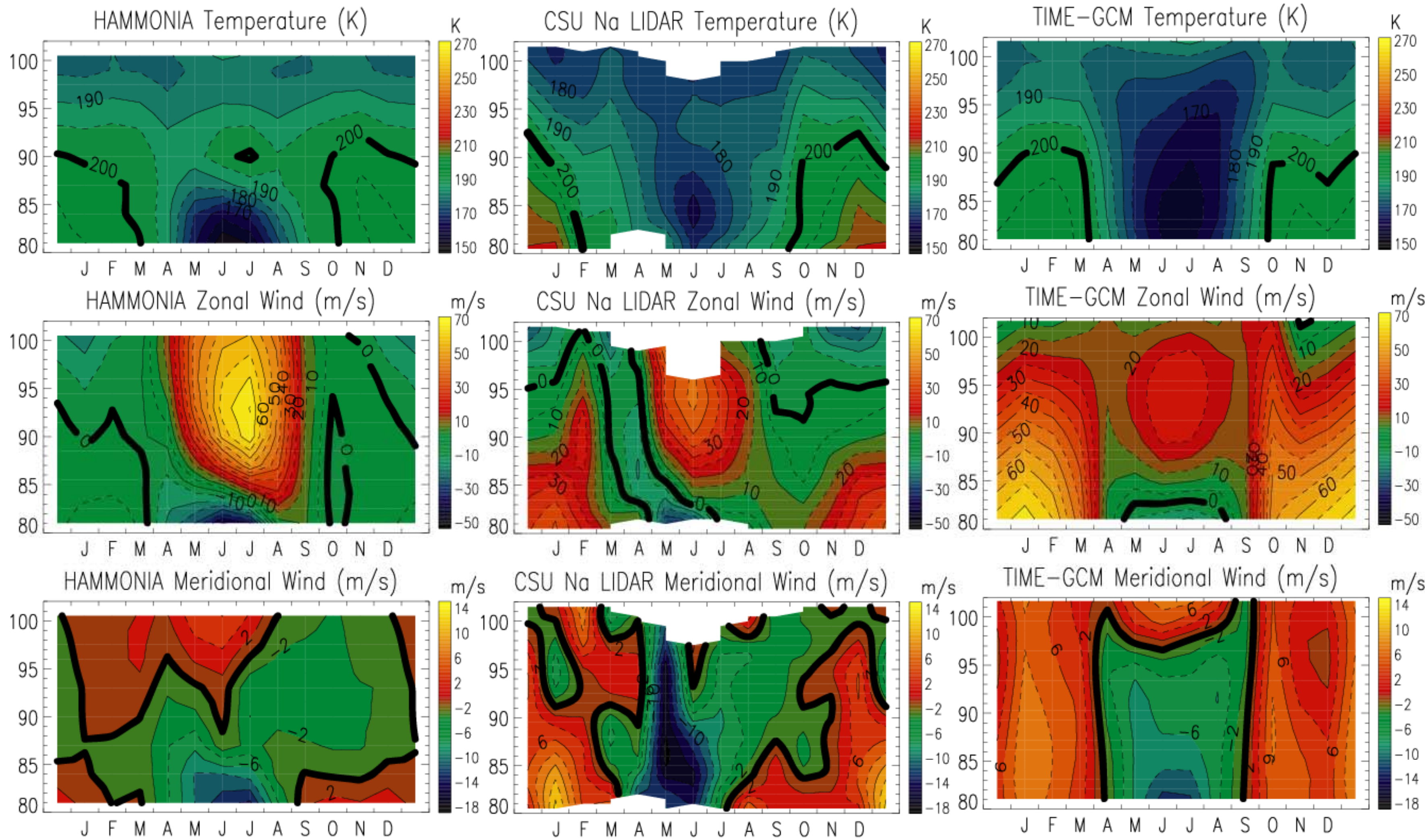

The observed results are in qualitative agreement with our current understanding of the mesopause region thermal and dynamical structure, with two-level mesopause , zonal wind switching directions and "residual" meridional flow (SP → WP).

Note: Difference from model less than that between models.

Long-term CSU lidar (1st light, Aug.,'89; regular, May '91)
Nightly average temperatures (1990 – March 2010)

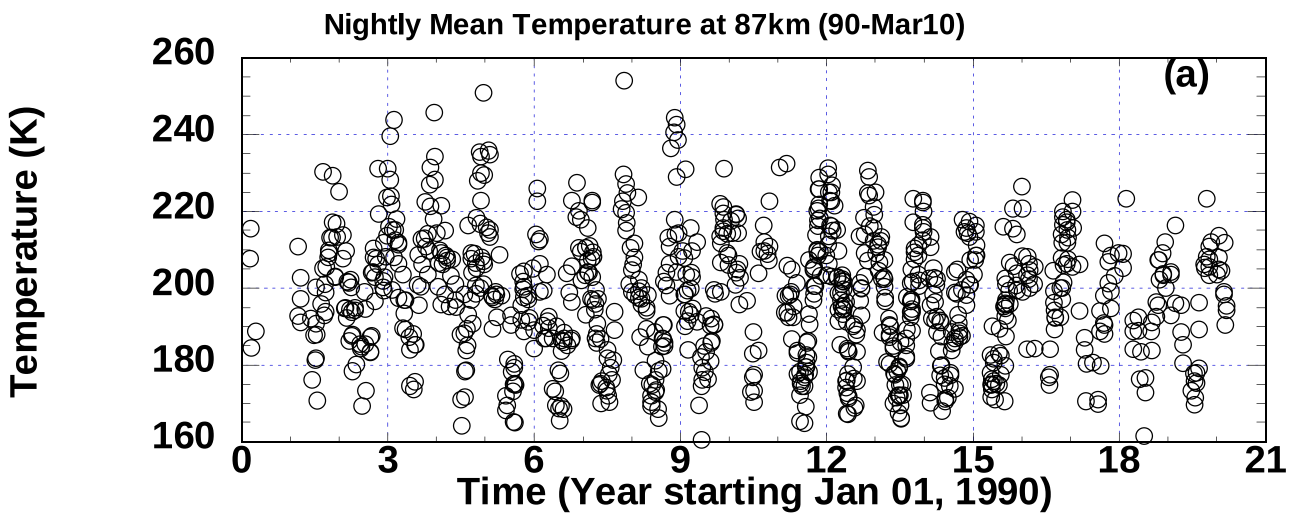

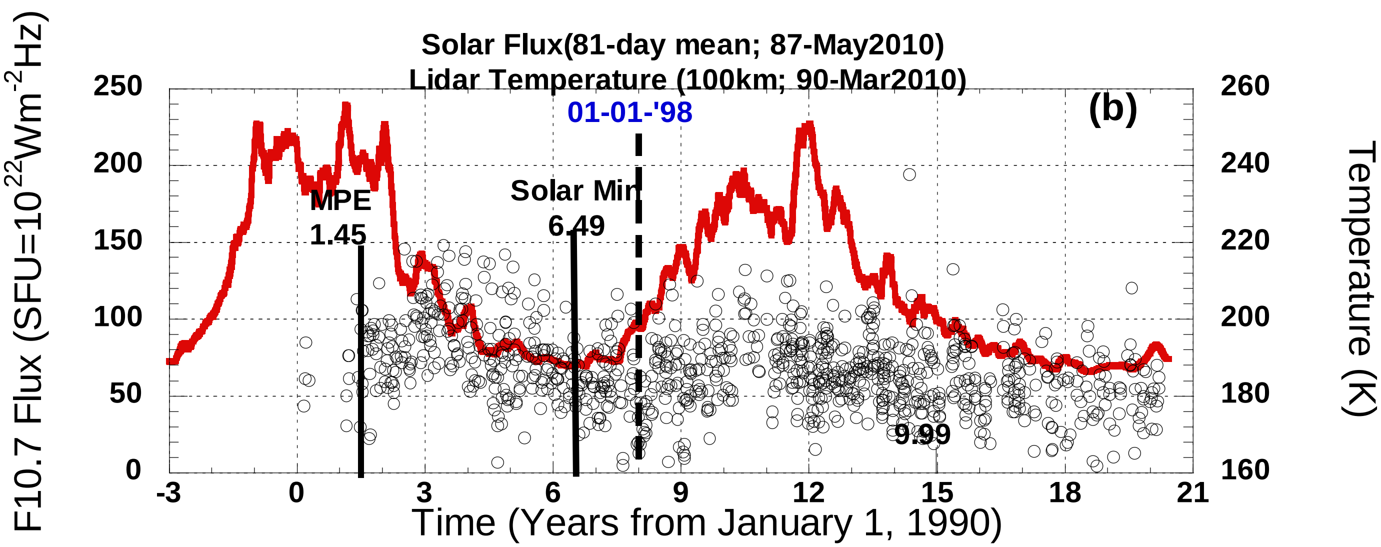

Main Results: Comparison between the analyses for the entire data set (1990-Mar2010) with "Pinatubo effect" accounted for (Red solid), removed (smaller red open) and ignored (large open).

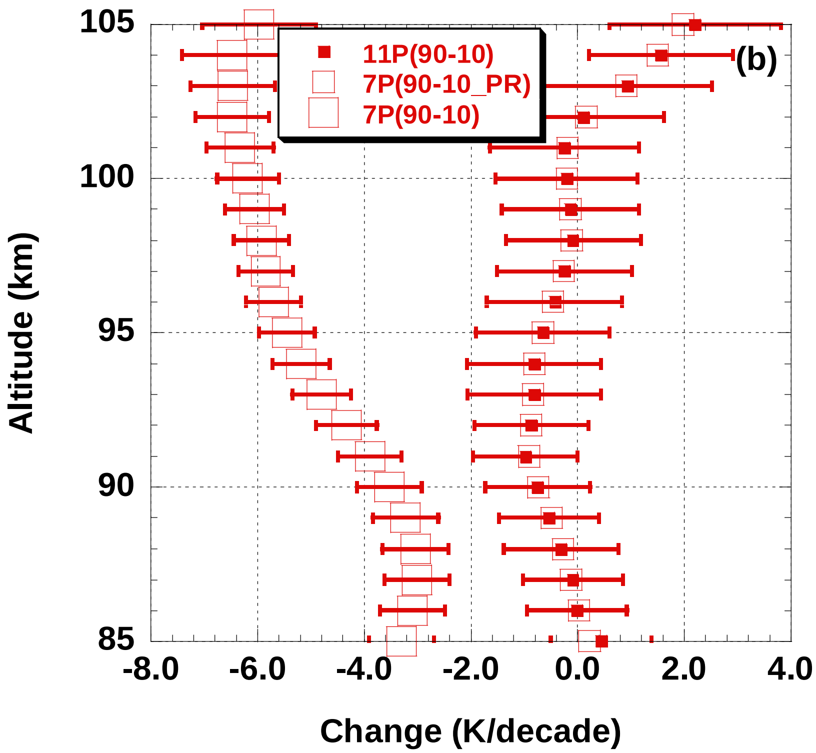

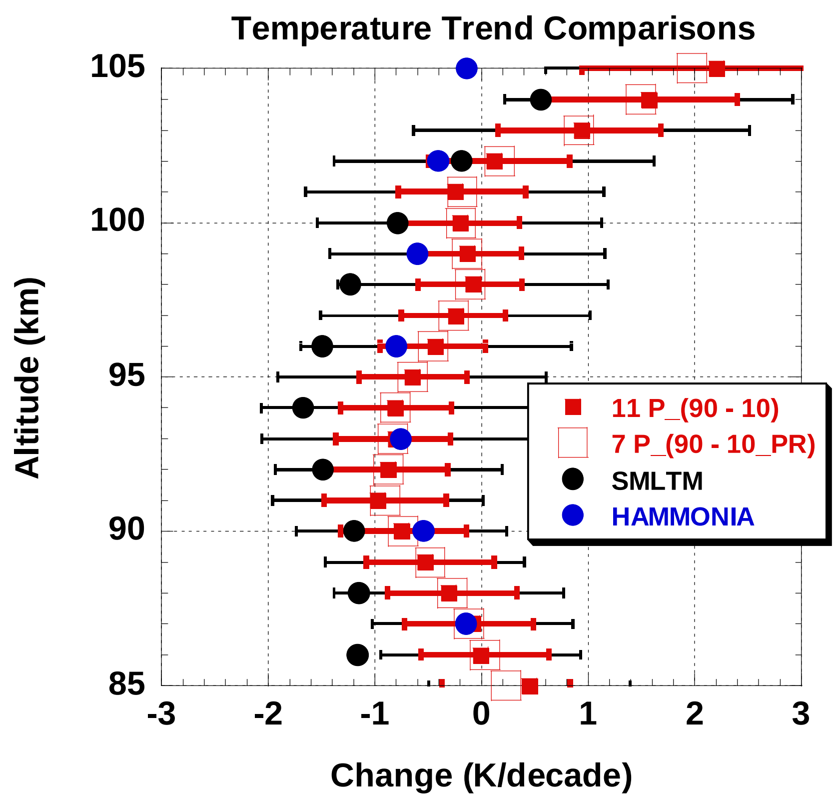

A mini resonance lidar workshop at CSU, August 2006

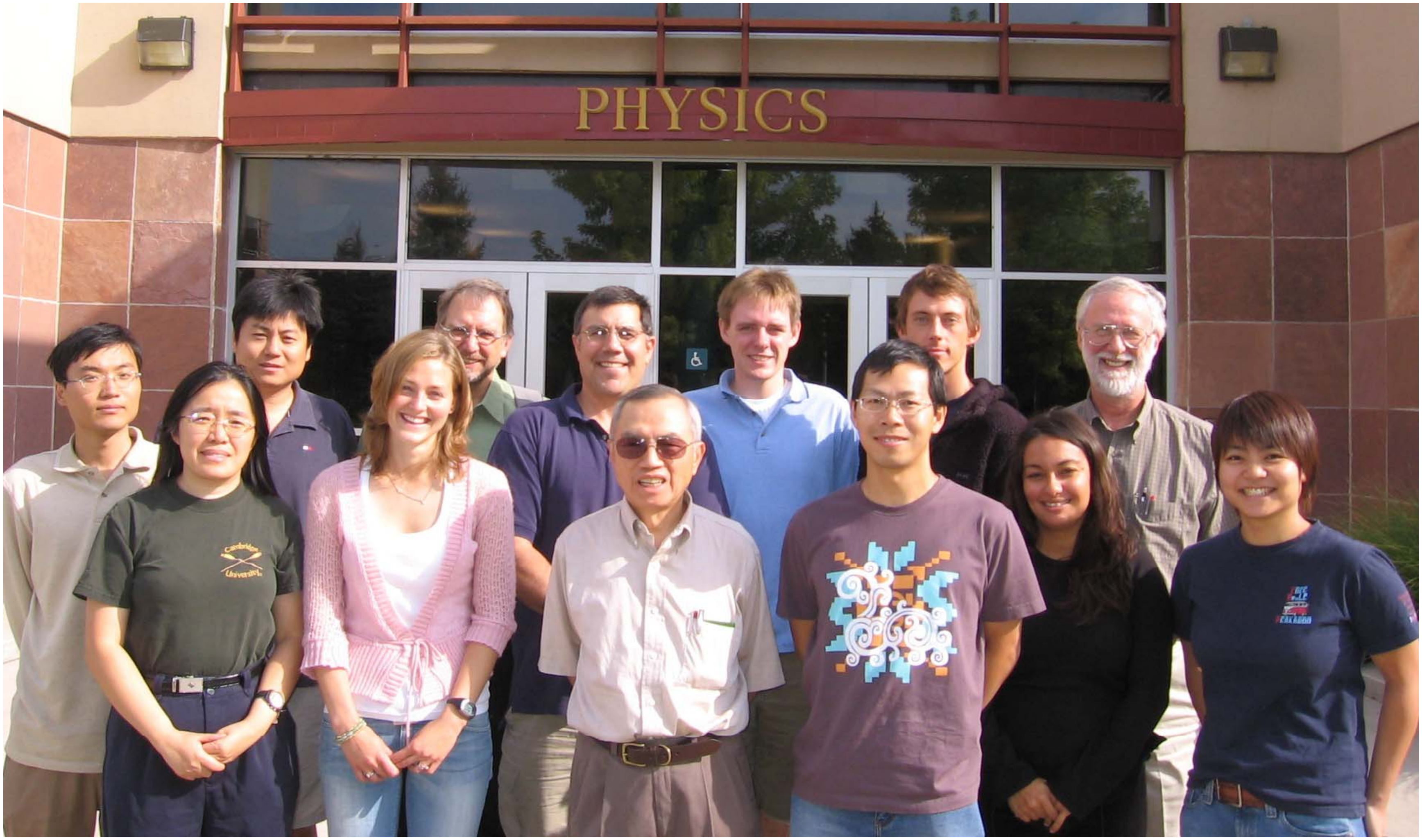

Group photo in front of Physics Department: in photo (from left to right) are Zhaoai Yan, Xinzhao Chu, Titus Yuan, Sandra Blindheim, Michael Gaussa, Phil Acott, Joe She, Sean Harrell, Wento Huang, Johannes Wiig, Paloma Farias, Dave Krueger, and Chihoko Yamashita. (Aug 06)

Atomic ^{56}Fe energy level diagram

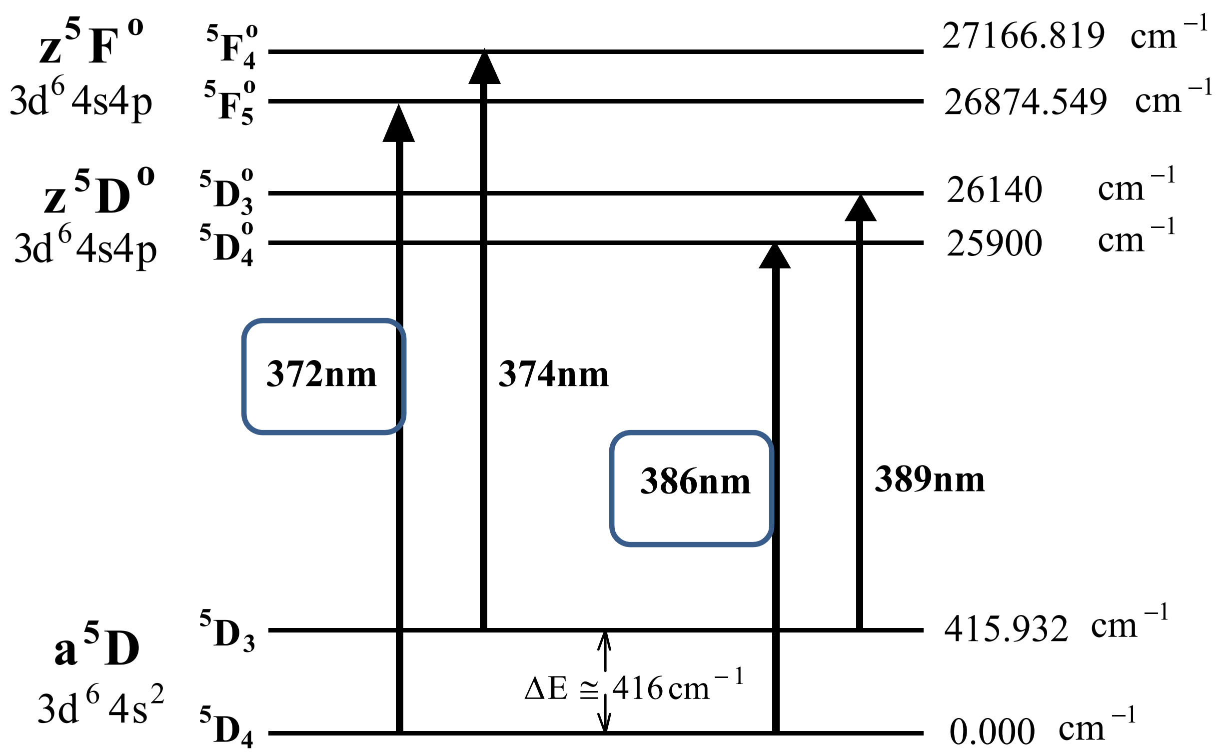

Boltzmann lidar uses both transitions from $^5D_4$ and $^5D_3$; latter weak

Narrowband Fe lidars (@ 386 or 372 nm) uses the Doppler-broadened transitions from the $^5D_4$ level; these are pursued by IAP and CU groups

Recent trends in full-diurnal-cycle metal lidars
Why Fe (UV) lidar and CW lidar for MLT studies?

Lidar trans. λ (nm)	Group (Reference)	Transition	Tuning/locking (Daytime filter)	Day Filter (divergence)
Pulsed Fe (386)	IAP (Höffner et al., OL,2009)	$(3d^64s^2\text{-}^5D_4)$ – $(3d^64s4p\text{-}^5D^o{}_4)$	Scan (Wavemeter)	Double-etalon (2 GHz) (50-54 μrad)
Pulsed Fe (372)	CU (Chu et al., ILRC, 2008/2010)	$(3d^64s^2\text{-}^5D_4)$ – $(3d^64s4p\text{-}^5F\ ^o{}_5)$	3 – freq (Doppler-free and Optical heterodyne)	Double-etalon (under development)
CW Na (589)	CSU/TMU/NIPR/CORA (Paper draft /HAIPER Prop)	D_2 $(3s^2\text{-}^2S_{1/2})$ - $(3s3p\text{-}^2P_{3/2})$	3 – freq (Doppler-free)	Faraday filter (2 GHz) (0.5 – 0.8 mrad)
Multiple l (386, Fe) (390-1, N_2^+) (393, Ca^+) (770, K)	TMU/NIPR (Abo/ Nakamura)	Fe $(3d^64s^2\text{-}^5D_4)$ –$(3d^64s4p$ - $^5D^o{}_4)$ KD_1 $(3s^2\text{-}^2S_{1/2})$ - $(3s3p\text{-}^2P_{1/2})$	N_2^+ and Ca^+ density only Fe and K also temperatures	Double etalon Faraday filter (under development)

Iron Lidar of IAP

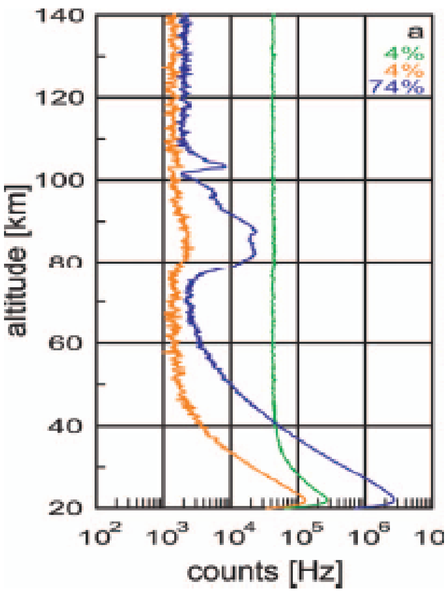

Left shows the signal and background near September noon (Sep 25, 07_13:15 UT) before, between, and after double etalons. Achievement of S/B ~ 10 is impressive.

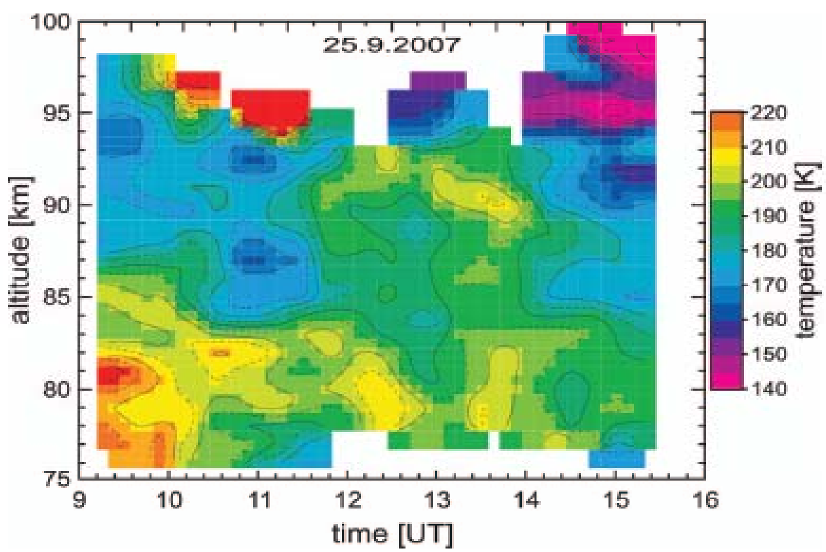

Fig. 5. Temperatures with 1 h and 1 km resolution. Uncertainty <5 K at peak of iron layer.

- Though with lower backscatter coefficient, the high number density produces backscatter signal comparable to Na. The narrow resonance line, operating at a field of view of 54 µrad yields an overall bandwidth of 2 GHz. This bandwidth along with the low sky background and strong Fraunhofer line at 386 nm yields much reduced background in observations under sunlit conditions as compared to current Na and K lidar.
- The center of the FOV is controlled to within 5 µrad, a daring undertaking.
- The fundamental at 772 nm provides Rayleigh-Mie scattering information.

(Hoffner and Lautenbach, 2009)

The MRI Fe Lidar

- The MRI iron lidar, led by Xinzhao Chu, is under construction . The instrument and science potential were briefed in the 24th ILRC.
- Doppler-free with a 372-nm external cavity diode laser (ECDL) and a hollow-cathode Fe discharge cell was also demonstrated (24th ILRC).
- The chirp (shift) of the pulses are monitored by optical heterodyne technique, pulse-to-pulse, the offset is removed by adjusting the seeder@ 744 nm (Chu and Huang, 25th ILRC).

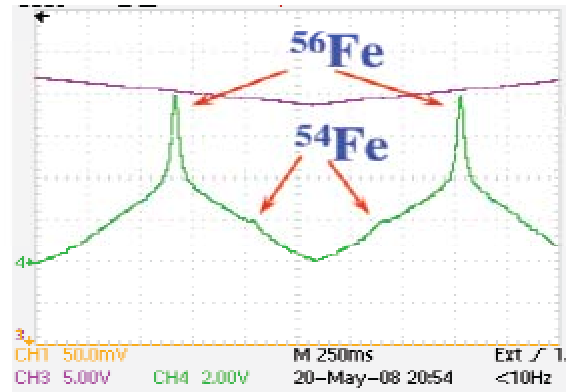

Figure 4. Detection of isotope line shift between ^{56}Fe and ^{54}Fe for the 372-nm absorption line

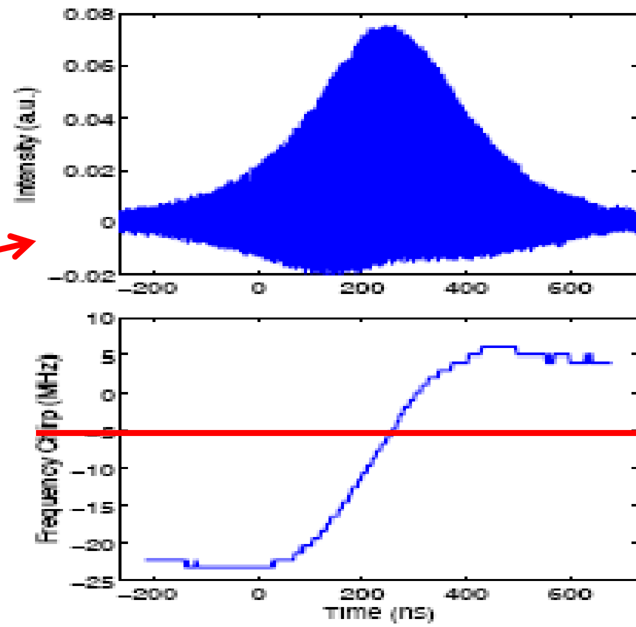

Figure 8. Another example of frequency chirp of the PARL pulse inferred from optical beat signal

A mesopause region temperature/wind sodium lidar with pseudorandom modulation continuous-wave (PMCW) technique at 589 nm
– She, Abo, Yue, Nagasawa, Nakamura

The CSU Na lidar system in 2002 with two beams pointing 30° off zenith, to the east and to the north. It is a small lidar with PA = 0.05 Wm^2/beam.

The uncertainties of CSU pulsed lidar at 1 h and 4 km resolution, between the minimum of 0.4 K (1.1 K) and 1.5 m/s (2.1 m/s) at the Na peak, ~91 km to the lower edge of 1.2 K (7.7 K) and 2.1 m/s (12.4 m/s) at 80 km and to the upper edge of 3.0 K (31.3 K) and 4.8 m/s (117 m/s) at 105 km for night (local noon) condition, can be scaled to PMCW lidar.

As shown, the ratio of the signal to noise ratio (S/N) of Pulsed/PMCW is conservatively estimated (with the same reciever FOV) to be 3.7 (4.9). Thus to achieve comparable results with a PMCW lidar using the same 35 cm diameter telescope, we need a CW laser of 20 W power, still a compact system compared to an 1 W pulsed system.

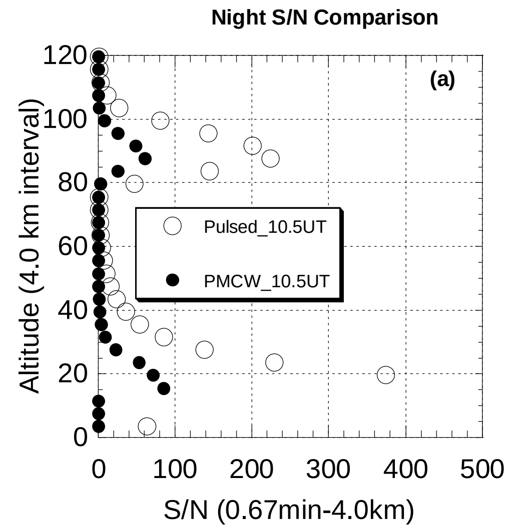

winter

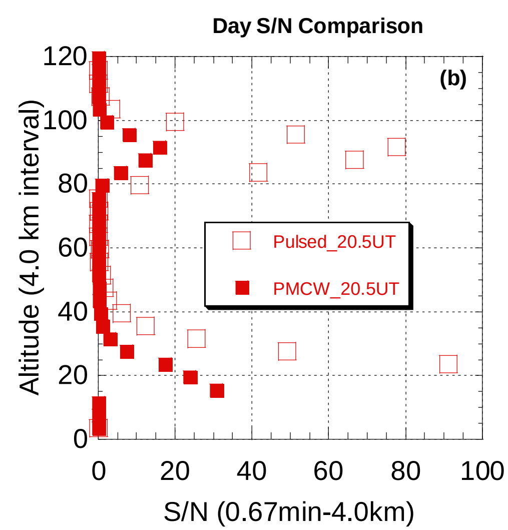

Targets for Multi-wavelength Resonance Scattering Lidar for Syowa (69° S) (NIPR/TMU/Antarctic lidar group)

	Trans. λ	Rec. λ	Measurement Parameter
Fe	385.99nm	←	Fe Density, (Temperature)
N_2^+	390.30nm	391.54nm	Aurorally Excited N_2 Ion
N_2^+	391.08nm	391.26nm	Thermospheric Temperature
Ca^+	393.36nm	←	Ca Ion Density
K	769.90nm	←	K Density, (Temperature)

All based on two newly developed Alexandrite lasers

Courtesy of Abo/Nakamura

For Details, please visit PF - 33

References

- Höffner, Josef and Jens Lautenbach, Daylight measurements of mesopause temperature and vertical wind with the mobile scanning iron lidar, Optics Letters, 34, 1351-1353 (2009).
- *Chu, X., W. Huang, J. S. Friedman, J.P. Thayer,* MRI: MOBILE FE-RESONANCE/RAYLEIGH/MIE DOPPLER LIDAR: PRINCIPLE, DESIGN, AND ANALYSIS, Proceeding ILRC24.
- S8P-02 *Chu, X., W. Huang*. FE DOPPLER-FREE SPECTROSCOPY AND OPTICAL HETERODYNE DETECTION FOR ACCURATE FREQUENCY CONTROL OF FE-RESONANCE DOPPLER LIDAR, Proceeding ILRC25, p. *969*.
- She, C.-Y., M. Abo, J. Yue, C. Nagasawa and T. Nakamura, A mesopause region temperature/wind sodium lidar with pseudorandom modulation continuous-wave (PMCW) technique at 589 nm (in preparation)
- M. Abo, T. Nakamura, M. Tsutsumi, et al., Development of Remote Controlled Lidar System and Multi-Wavelength Resonance Scattering Lidar System at Syowa Station, 27th Japanese Laser Sensing Symposium, No.PB-3, 2009.

Conclusion

- Metal lidars of various type have proven to be effective for the study of mesosphere and lower thermosphere (MLT) science since 1985, about 25 years ago.
- The CSU Na lidar is small lidar (35 cm dia. Telescope, 1 W for two beams), measuring T, U, V simultaneously with full-diurnal-cycle observation capability. Its potential for MLT science studies, not otherwise possible without a lidar has been fully demonstrated by dynamics studies with time scales ranging from 30 min to tens of years, for the study of gravity waves (GWs), tidal waves, planetary wave and T, U, V climatology, as well as long-term effects (volcanic response, solar cycle effect and temperature trends). Shorter period PWs possible with a larger lidar.
- Due to the desire to reduce the reception of sky background, Fe lidar at 386 and 272 nm are being developed. The desire for a compact lidar transmitter, the PMCW Na lidar, pioneered in Japan, is under investigation; it is potentially suitable for airborne and/or spaceborne observations.